Journal of Hazardous Materials, 15 (1987) 343–364
Elsevier Science Publishers B.V., Amsterdam — Printed in The Netherlands

THE EVAPORATION OF VOLATILE LIQUIDS

PETER I. KAWAMURA and DONALD MACKAY

Department of Chemical Engineering and Applied Chemistry, University of Toronto, Toronto, Ontario M5S 1A4 (Canada)

(Received January 18, 1986; accepted in revised form August 18, 1986)

Summary

Two models have been developed to estimate the evaporation rate of volatile and non-volatile liquids resulting from ground spills. Both models are based on steady state heat balances around the chemical pool and include the effects of solar insolation, evaporative cooling, and heat transfer from the ground. The simpler of the two, the "direct evaporation" method, estimates the evaporation rate directly from available physical-chemical data. The second model, the "surface temperature" method, determines the surface temperature of the evaporating pool by an iterative procedure. This temperature is then used to estimate the evaporation rate.

Experiments are described in which the evaporation rates of seven volatile chemicals were measured from pans under known meteorological conditions, including summer and winter temperatures. The two models and the experimental evaporation rates were in satisfactory agreement, i.e. an average difference of 19% for the direct evaporation method, and 13% for the surface temperature method. It is concluded that either model can be used to estimate evaporation rates under actual spill conditions.

1 Introduction

Accidental spills of hazardous and toxic chemicals can present a serious risk to the public's safety and to the environment. An immediate concern is the generation of an excessive chemical vapor concentration downwind of the spill, which may cause health and fire hazards. To establish this exposure concentration, the source strength, or the evaporation rate of the chemical must be determined. This evaporation rate is also useful in determining the approximate time required for complete evaporation, which is an important factor in implementing proper mitigative procedures. This study is concerned with the prediction of the evaporation rate of pure volatile liquid chemicals resulting from ground spills.

The driving force for the evaporation process is the vapor pressure of the chemical, evaluated at the surface of the chemical pool. This requires a knowledge of the surface temperature of the evaporating pool, which is a function of many variables, including radiative heat transfer by solar insolation, evapo-

0304-3894/87/$03.50

rative cooling, and direct heat transfer between the chemical pool and air, and between the pool and ground. The effects of the evaporative cooling and direct heat transfer terms are most significant for volatile chemicals. This is due to the depression of the surface and pool temperatures relative to the ambient temperature as a result of the evaporative cooling of the chemical. For example, an experiment [1] performed under environmental conditions in which pentane was allowed to evaporate from a flat pan showed that the evaporation rate calculated by neglecting this cooling effect over-estimated the experimental evaporation rate by approximately a factor of four. Therefore, this effect must be incorporated in the formulation of any reliable evaporation rate model.

Terrestrial evaporation models have been developed by several workers [2–7]. Of these, the majority [2–6] cannot be applied with confidence to volatile chemicals since they neglect the evaporative cooling effect, as well as other effects such as solar insolation. In the Ille and Springer model [7], these effects are incorporated but its general applicability is limited by the difficulty of obtaining some of the input parameters required. This model is also relatively complicated and involves using a long computer program.

This study was performed to develop and verify a simple formula or procedure which can predict with acceptable accuracy the evaporation rate of pure liquid chemicals resulting from ground spills under various environmental conditions.

2 Theoretical principles

An energy balance for a chemical pool under environmental conditions may be written in the following form, each term having dimensions of kJ/m^2 h

$$Q_{sol} + Q_{atm} - Q_{sur} - Q_{ev} + Q_{sen} + Q_{grd} = Q_t \quad (1)$$

where Q_{sol} is the net solar radiation (corrected for the amount reflected from the surface), Q_{atm} is the long-wave radiation from the atmosphere absorbed by the pool, Q_{sur} is the long-wave radiation emitted by the pool, Q_{ev} is the evaporation energy, Q_{sen} is the net sensible heat conducted into the pool from the atmosphere, Q_{grd} is the heat conducted from the ground, and Q_t is the increase in energy stored in the pool. These terms are illustrated in Fig. 1 and are described individually in the following paragraphs.

The net solar insolation may be estimated from Raphael's [8] solar insolation curves which are plots of the net solar radiation on a water surface (corrected for reflectivity) as a function of cloud cover and solar altitude. These can be approximated by the relationship

$$Q_{sol} = 4000\ (1 - 0.0071\ C^2)\ (\sin SA - 0.1) \quad (2)$$

where C is the cloud cover factor in tenths (0 for clear day, 10 for complete cloud cover), and SA is the solar altitude, in degrees. This equation has units

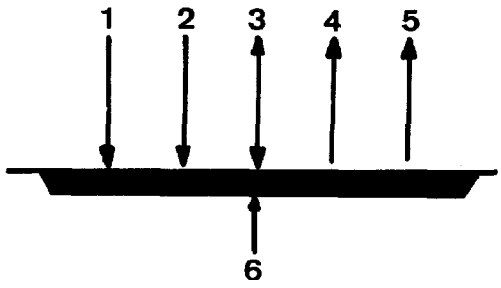

Fig. 1. Steady state energy budget for an evaporating pool: 1-net solar radiation, 2-atmospheric radiation, 3-sensible heat, 4-emitted radiation, 5-evaporation energy, 6-ground conduction.

of kJ/m^2 h, and is valid only for sinSA greater than 0.1. For values between 0 and 0.1, solar insolation is very small and can be assumed to be negligible. Equation (2) showed good agreement in field experiments when compared against measurements obtained from a pyranometer [1]. In the interest of simplicity, this equation is applied to the various chemicals without correction for the individual reflectivities. A sample calculation is illustrated in the Appendix.

The long-wave energy exchange terms are calculated from the Stefan–Boltzmann radiation law

$$Q_{atm} = (1-r)\, B\sigma\, T_a^{\,4} \tag{3}$$

$$Q_{sur} = e\sigma\, T_s^{\,4} \tag{4}$$

where σ is the Stefan–Boltzmann constant (2.04×10^{-7} kJ/m^2 h K^4), r is the reflectivity of the surface with respect to long-wave radiation, e is the emissivity, and T_a and T_s are the absolute temperatures of the air and surface of the pool, respectively. In this study, the values for water [8] of 0.03 for r and 0.97 for e are used. The term B is defined as the atmospheric radiation factor, which Raphael [8] plotted as a function of cloud cover and vapor pressure of water in air, which can be determined from the relative humidity of the atmosphere. This is presented in Fig. 2.

The energy required for evaporation is the product of the evaporation rate and the heat of vaporization. The evaporation rate per unit area is

$$E = k\, M\, P\,(T_s)/RT \tag{5}$$

where k is the mass transfer coefficient (m/h), M is the molecular weight, $P(T_s)$ is the vapor pressure of the chemical evaluated at the surface of the pool (Pa), R is the gas constant (8.314 Pa m^3/mol K), T is the absolute temperature, and E is the evaporation rate (g/m^2 h). The mass transfer coefficient was correlated by Mackay and Matsugu [9]

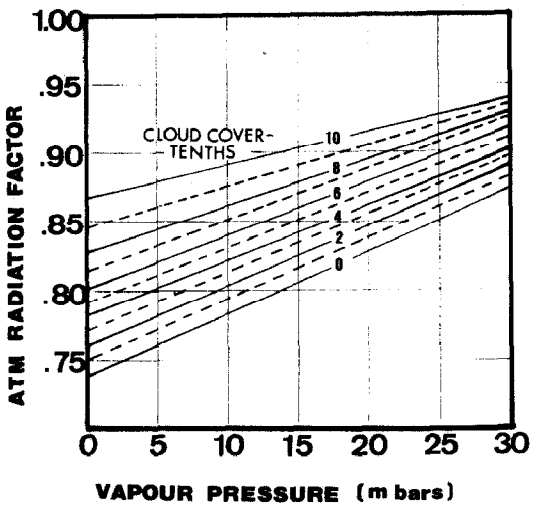

Fig. 2. Atmospheric radiation factor (Adapted from Raphael [8]).

$$k = 0.029\ U^{0.78}\ X^{-0.11}\ Sc^{-0.67} \tag{6}$$

in which U is the 10 m wind speed (m/h), X is the pool diameter, or the downwind length of the pool (m), and Sc is the chemical's Schmidt number in the air phase.

The Schmidt number is a dimensionless group which is the ratio of momentum and mass diffusivities. It is evaluated by dividing the kinematic viscosity of air by the diffusivity of the chemical in air. It generally has a value of 1.0 to 2.5.

Therefore, the evaporation energy is:

$$Q_{ev} = E\ H_v / M \tag{7}$$

where H_v is the heat of vaporization (kJ/mol).

Sensible heat transfer between the air and the pool occurs as a result of a difference in temperature between the two phases:

$$Q_{sen} = U_{liq}\ (T_a - T_s) \tag{8}$$

where U_{liq} is the heat transfer coefficient (kJ/m^2 h K), which can be estimated from the heat and mass transfer analogy:

$$U_{liq} = k\ \rho_a\ C_{p_a}\ (Sc/Pr)^{0.67} \tag{9}$$

in which ρ_a is the molar density of air (mol/m^3), C_{p_a} is the heat capacity of air (kJ/mol K) and Pr is the Prandtl number. In this study, typical values of 0.72 were used for the Prandtl number and 1.2 for the product of the molar density and the heat capacity of air, i.,e. 42 mol/m^3 and 0.029 kJ/mol K, respectively.

Conduction of heat from the ground may be evaluated by assuming that the

ground is a semi-infinite slab of initial uniform temperature, T_i. The average heat flux at the chemical–ground interface over a certain time period is [10]:

$$Q_{grd} = (2\,k_{grd}/\theta)\ (\theta/\pi\alpha)^{0.5}\ (T_i - T_{gs}) \tag{10}$$

in which θ is the time after the spill (h), k_{grd} is the thermal conductivity of the ground (kJ/m h K), α is the thermal diffusivity of the ground (m^2/h), and T_{gs} is the surface temperature of the ground. α is $k_{grd}/(C_{p_g}\rho_g)$ where C_{p_g} is the heat capacity of the soil and ρ_g its density with units such that their product has units of kJ/m^3 K. This ground conduction effect will be most significant for volatile chemicals due to the large temperature driving force between the pool and the ground, created by the evaporative cooling of the chemical. The heat transfer from the ground will also decrease with time, as the temperature of the ground approaches the pool temperature. From eqn. (10), a time dependent heat transfer coefficient, h_{grd}, can be defined:

$$h_{grd} = 2\,k_{grd}\ (\theta/\pi\alpha)^{0.5}/\theta \tag{11}$$

It is desirable to write eqn. (10) in terms of the same temperature driving force as in eqn. (8). Since the initial temperature of the ground is not usually measured, it is acceptable for the purposes of this study to equate it to the air temperature. The surface temperature of the pool is introduced in place of the surface temperature of the ground by identifying an overall heat transfer coefficient, U_{grd}:

$$U_{grd} = 1/[(1/h_{grd}) + (1/h_{liq})] \tag{12}$$

in which h_{liq} is the heat transfer coefficient that accounts for the thermal resistance from the surface of the ground to the surface of the chemical pool. We suggest that this liquid heat transfer coefficient be estimated from:

$$h_{liq} = k_{liq}/(\phi\bar{d}) \tag{13}$$

in which k_{liq} is the thermal conductivity of the chemical (kJ/m h K), $\bar{d}$ is the average depth of the pool over the entire course of evaporation (i.e. half the initial depth), and ϕ is a "liquid resistance" factor which takes into account the relative roles of heat transfer by conduction and turbulence. If only conduction occurs ϕ will equal unity. If eddy transfer occurs h_{liq} is larger and ϕ is smaller than unity. A correlation for ϕ is derived later from experimental data, and is discussed in Section 5. This correlation is

$$\phi = 1/\{1 + \exp[-0.06(t_{bp} - 70)]\} \tag{14}$$

where t_{bp} is the normal boiling point of the chemical (°C).

The thermal contribution from the ground may now be written as:

$$Q_{grd} = U_{grd}\ (T_a - T_s) \tag{15}$$

3 Evaporation models

Two relatively simple evaporation models were assembled to predict the evaporation rate from ground spills. These are termed the "direct evaporation" method and the "surface temperature" method. Both models are based on a quasi steady state heat balance around the chemical pool, which includes the effects of solar insolation and evaporative cooling. The required parameters for the models, such as solar radiation and heat transfer coefficients are determined from equations and figures presented earlier.

3.1 Direct evaporation method

This model is based on the approach taken by Penman [11,12] to estimate the natural evaporation rate of water. Modifications have been made to adapt this approach to the evaporation of chemicals under environmental conditions.

Bowen's ratio, B_o, which is the ratio of the energy conducted to the pool as sensible heat, to the energy lost by evaporation is often used in water evaporation studies. This ratio may be written as:

$$B_o = Z\ (T_a - T_s)/(P_s - P_a) \tag{16}$$

where P is the partial pressure of the chemical (or water) with subscripts designating at the surface (s), and the bulk of the air (a).

This ratio is useful in the development of an evaporation model but it cannot be utilized in this form, since it contains terms dependent on the unknown surface temperature. We introduce expressions for these terms based on simplifying assumptions, existing theory, and correlations, which result in an explicit relationship between the evaporation rate and terms which can be easily determined.

The term Z in the Bowen's ratio may be evaluated from eqns. (5), (7–9), and (15), and by noting that the density of air is the atmospheric pressure divided by the gas constant and the absolute temperature

$$Z = P_{atm}\ C_{p_a}\ (Sc/Pr)^{0.67}/H_v + U_{grd}\ RT/k\ H_v \tag{17}$$

This equation can be simplified by treating the atmospheric pressure (101,000 Pa), heat capacity of air (0.029 kJ/mol K), and the Prandtl number (0.72) as constant:

$$Z = 3650\ (Sc)^{0.67}/H_v + U_{grd}\ R\ T/k\ H_v \tag{18}$$

To eliminate the surface temperature, T_s, in the Bowen's ratio, the following assumption is made:

$$S = (dP^*/dT)_{T_a} \approx [P(T_s) - P(T_a)]/(T_s - T_a) \tag{19}$$

where S is the slope of the vapor pressure curve for the chemical, and P^* is the saturation vapor pressure. The slope is approximated by evaluating the deriv-

ative of the vapor pressure equation at the air temperature. It should be noted that since the concentration of the chemical in the bulk air phase is usually close to zero, the term P_a in the Bowen's ratio is negligible. This ratio becomes:

$$B_o = -(Z/S)\ [1-P(T_a)/P(T_s)] = (Q_{grd}+Q_{sen})/Q_{ev} \tag{20}$$

A term, E_r is defined which can be viewed as the rate at which the chemical can be evaporated as a result of solar insolation:

$$E_r = Q_{sol}\ M/H_v \tag{21}$$

This model neglects the long-wave radiation terms since the term Q_{sur} cannot be determined. However, this term is assumed to be approximately equal to the atmospheric radiation, Q_{atm}, under most conditions. Regardless of the magnitudes of these individual terms, the long-wave radiation exchange, $(Q_{atm}-Q_{sur})$, is assumed to be small compared to the other energy terms in the heat balance.

A second term, E_a is introduced as the liquid evaporation rate assuming that the pool surface temperature equals the air temperature. Since evaporation rate is proportional to vapor pressure, E_a is related to the actual evaporation rate E as

$$E_a/E = P(T_a)/P(T_s) \tag{22}$$

Equations (1) (with Q_t and (Q_{atm} - Q_{sur}) assumed to be zero), and eqns. (20–22) can be solved for E. This is done by eliminating $P(T_a)/P(T_s)$ from eqn. (20) using eqn. (22); eliminating $(Q_{grd}+Q_{sen})$ from eqn. (1) using eqn. (20); eliminating Q_{sol} by eqn. (21); and replacing Q_{ev} by $E\,H_v/M$; to give, after some rearrangement

$$E = E_r\ S/(S+Z) + E_a Z/(S+Z) \tag{23}$$

If the ratio Z/S is designated β then eqn. (23) becomes

$$E = E_r\ 1/(1+\beta) + E_a\beta/(1+\beta) \tag{24}$$

The key variable is thus β which controls the relative contributions of E_r and E_a. If β is small compared to unity E approaches E_r, while if β is larger E approaches E_a.

The group β or Z/S can be shown to be a function of vapor pressure. The heat of vaporization H_v is related to the slope of the vapor pressure–temperature curve as follows from the Clausius–Clapeyron equation

$$\mathrm{d}\ln P^*/\mathrm{d}T = (1/P^*)\ \mathrm{d}P^*/\mathrm{d}T = (1/P^*)S = H_v/RT^2 \tag{25}$$

It follows from eqns. (18), (19), and (25) that

$$\beta = Z/S = [3650\ Sc^{0.67} + (U_{grd}\ RT/k)]\ RT^2/P^*\ H_v^{\,2} \tag{26}$$

and is thus approximately inversely proportional to vapor pressure.

A substance of high vapor pressure (e.g. pentane) will have a small β, and E tends to be dominated by E_r. Such substances tend to have large evaporative cooling effects (i.e. $(T_a - T_s)$ is large). Low vapor pressure, high boiling point liquids will have a larger β and E is dominated by E_a, the air–pool temperature difference being small.

The advantage of this model is that it is simple and requires no iteration. The working equations are summarized and illustrated in the Appendix.

3.2 Surface temperature method

This model determines the surface temperature of the pool based on the steady state energy balance (eqn. (1) with $Q_t = 0$). This temperature is then used to calculate the evaporation rate using eqn. (5).

Equation (1) can be rearranged to give

$$Q_{sol} + Q_{atm} + T_a(U_{liq} + U_{grd}) = T_s\,(U_{liq} + U_{grd}) + k\,H_v\,P(T_s)/RT_s + e\,\sigma\,T_s^4 \quad (27)$$

The left side of eqn. (27) consists of terms which can be evaluated, whereas the right side contains terms dependent on the unknown surface temperature. This equation may be solved for the surface temperature by standard root determining methods such as the Newton's method, which was used in this study.

This procedure is best suited for a computer but the program required is very short and simple. Despite having to use a computer or a programmable calculator in this method, it has the advantage of including all the energy exchange terms that are present in the overall energy balance.

Again the procedure is illustrated in the Appendix.

4 Experimental

Two sets of evaporation experiments were performed at the Environment Canada Atmospheric Environment Services experimental site in Woodbridge, Ontario, in which the selected chemicals were allowed to evaporate from a flat circular pan under various environmental conditions. All experiments were conducted during daylight.

In the first set of experiments, the effect of ground conduction on the evaporation rate was eliminated by placing a styrofoam board under the evaporation pans. The pans, with the inner surface painted black, were of diameters, 0.61 and 0.91 m and depth 5 cm. The choice of the pan size used in specific experiments was based on the relative volatility of the chemical and the prevailing atmospheric conditions. The following chemicals were used: toluene, cyclohexane, n-hexane, methanol, pentane, dichloromethane, and Freon 11 (trichlorofluromethane). The evaporation rate was measured by a device which

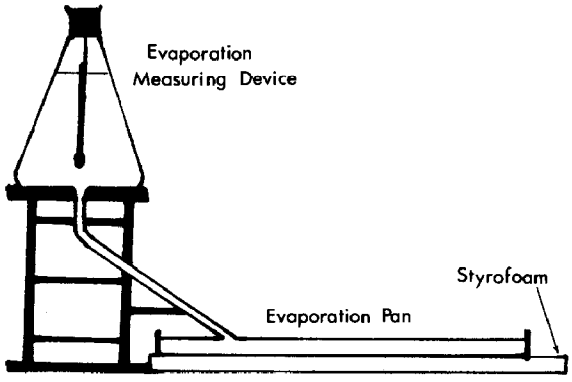

Fig. 3. Schematic diagram of apparatus for experiments without ground conduction.

consisted of a 6 L glass reservoir, initially filled with the chemical at ambient temperature, and a glass tube, which served to connect the reservoir and the evaporating chemical in the pan. This device maintained a constant level of chemical in the evaporation pan by replacing the evaporated chemical by additions of chemical from the reservoir. The evaporation rate was determined by observing the volume changes in the reservoir over the duration of the experiment. This apparatus is illustrated in Fig. 3.

In the second set of experiments, a pan, 0.46 m in diameter with a height of 10.2 cm was used. The pan was filled to a depth of 5 cm with sand of approximate size 0.05–1.0 mm, and was then partially buried in the ground so that the surface of the sand was just slightly higher than ground level. Before the experiment, the sand was saturated with water to avoid sorption of the chemical into the sand matrix. Either 4 or 7 L of the chemical, with the same initial temperature as that of the surroundings, were then introduced onto the sand surface. The chemicals used in these experiments were: pentane, toluene, hexane, cyclohexane, and Freon 11. The chemical was allowed to evaporate without interruption until either the depth of chemical remaining in the pan was less than 1 cm; or the experimental duration became excessively long. The evaporation rate was determined by measuring the volume of chemical remaining in the pan, at the termination of the experiment.

In addition to the evaporation rate, the bulk pool and surface temperatures were measured for both sets of experiments. The latter was accomplished by placing a copper–constantan thermocouple at the surface of the pool. This device was also used to measure sand temperatures at three different depths in the ground conduction experiments. Atmospheric data, such as air temperature, cloud cover, average wind speed, and relative humidity were also recorded, the latter from the weather office. The surface wind speed, which was measured using a cup-counter anemometer, was adjusted to a height of 10 m by using the universal velocity distribution equation with the appropriate roughness length

parameter. In the first set of experiments, all data, including the evaporation rate, were averaged over a time interval of 30 to 60 min for each experiment after "steady state" conditions were reached. Steady state condition was defined as the time after initial filling of the pan with the chemical when the pool temperature did not change by a rate greater than 2°C over a five minutes period. In the second set of experiments, the data were averaged over the entire duration of the experiment.

The recorded data, with the exception of the surface and pool temperatures, were used as input data to the two evaporation models. The model predictions were then compared to the experimental evaporation rate. Data not used in the model predictions, such as the surface temperature of the pool, was used instead to calculate the experimental mass transfer coefficient, which was tested against the mass transfer coefficient correlation (eqn. 6). Heat transfer due to the introduction of the chemical from the reservoir in the first set of experiments was estimated by computing the "external" source/sink of heat as a result of the difference between the bulk pool temperature and the reservoir temperature. This energy term was added to the solar insolation term in both evaporation models. The sand temperatures obtained from the second set of experiments were used to determine the liquid resistance factor (eqn. 14).

5 Results and discussion

5.1 Evaporation experiments without ground conduction

These experimental results (given in Table 1 in increasing order of chemical volatility) were compared to the evaporation rates predicted by the direct evaporation and surface temperature models. It was found that in most experiments, a quasi steady state was reached within 15 min of commencement of the experiment. The experimental and model predictions are compared in Fig. 4.

The results suggest that both the direct evaporation method and the surface temperature method predict evaporation rates which generally agreed well with the experimental evaporation rates under both summer and winter conditions. The difference between the predicted and the experimental rates varied from 0 to 40%, with an average of 17% for the direct evaporation method and 1 to 32%, with a 12% average for the surface temperature method. This error is judged to be acceptable for models applied under environmental emergency conditions.

As expected, the surface temperature model was more accurate than the simpler direct evaporation model. Table 1 reveals that the two predictions for moderately volatile chemicals (experiment no. 1–7) were excellent, with the exception of experiment no. 2. However, the model predictions for experiments involving very volatile chemicals (experiment no. 8–17) were, in general, not as successful. This is particularly apparent in the direct evaporation model,

TABLE 1

Summary of evaporation rate (kg/m^2 h) results and model predictions for experiments without ground conduction

Exp.	Chemical	Air Temp., °C	Model predictions				Experimental
			Direct evaporation	(% dif.)	Surface temperature	(% dif.)	
1	Toluene	21	4.97	(11)	4.63	(3)	4.49
2	Toluene	29	4.63	(37)	4.46	(32)	3.39
3	Cyclohexane	24	6.41	(9)	6.21	(5)	5.89
4	Cyclohexane	25	6.23	(6)	6.13	(4)	5.89
5	Hexane	−5	5.68	(2)	5.65	(2)	5.55
6	Hexane	22	10.90	(0)	13.00	(19)	10.88
7	Methanol	7	2.35	(1)	2.67	(4)	2.55
8	Dichloromethane	−6	7.26	(23)	9.57	(1)	9.49
9	Dichloromethane	1	6.69	(11)	6.07	(19)	7.53
10	Dichloromethane	21	13.91	(15)	19.20	(18)	16.27
11	Dichloromethane	25	15.60	(13)	19.90	(11)	17.98
12	Pentane	1	7.22	(31)	8.39	(20)	10.52
13	Pentane	5	4.19	(39)	5.67	(17)	6.84
14	Pentane	7	4.97	(39)	6.64	(18)	8.13
15	Pentane	9	6.18	(40)	8.30	(20)	10.41
16	Freon 11	0	29.67	(10)	38.22	(16)	33.01
17	Freon 11	17	28.79	(18)	35.79	(2)	34.93

which underpredicted the evaporation rates for all of these experiments. This underestimation of the evaporation rates can be attributed mainly to the assumption that the slope of the vapor pressure curve for the chemical is linear. The error introduced from this approximation is most significant for very volatile chemicals due to the large temperature difference between the surface and the air temperature.

Comparison was also made between the experimental mass transfer coefficient and the mass transfer correlation (eqn. 6). The difference between the two coefficients ranged from −35% to +47%, relative to the experimental value. There were no observable trends with respect to the chemical or the magnitude of the wind speed on the predictive behavior of the correlation.

5.2 Ground conduction effect

The first objective in performing evaporation experiments with ground conduction was to establish and quantify this energy term for the evaporation models. The approach was to correlate the experimental liquid resistance factor with chemical properties. This correlation would subsequently be used in the two evaporation models to predict the evaporation rates of these experiments.

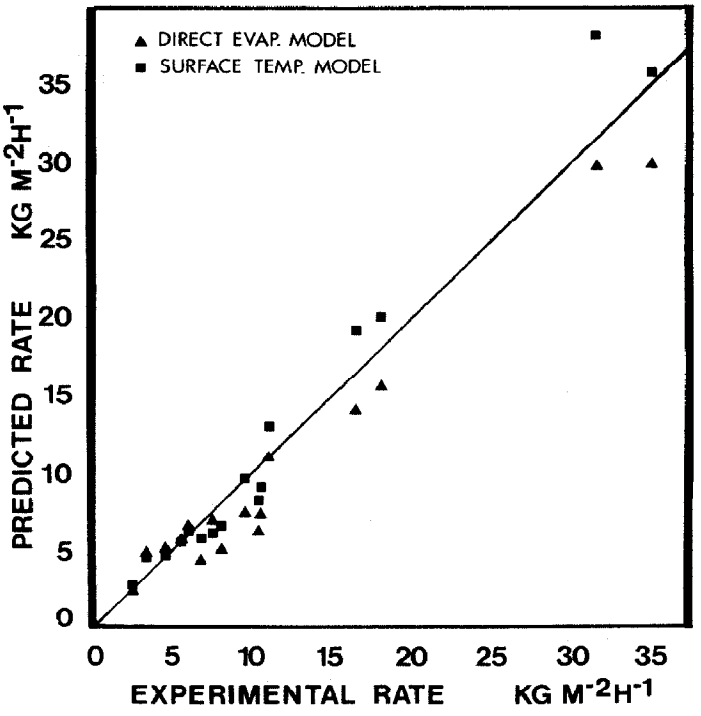

Fig. 4. Comparison of model predictions and the experimental evaporation rate.

The measured chemical surface and the initial and final sand temperatures (averaged over the sand depth) were used to calculate the experimental liquid resistance factor, ϕ, using eqns. (11–13) and eqn. (15). This factor, when multiplied by the actual depth of the pool gives the effective depth associated with the thermal resistance in the pool. These values were plotted against the normal boiling point of the chemical, which is presented in Fig. 5. This resulted in a relationship identified by eqn. (14) for the liquid resistance factor.

Although the number of experiments performed to determine this relationship is small, the liquid resistance factor, identified by eqn. (14), ensures a value of ϕ between 0 and 1, as required, for all boiling points. The physical basis for this correlation, which assigns a value close to unity for the relatively higher boiling point chemicals, and a very small value for low boiling point chemicals lies in the induced turbulence that exists in the chemical pool. For highly volatile low boiling point chemicals, ϕ is very small and heat transfer is rapid due to the turbulence and the vertical mixing created in the pool by the high evaporation rate, whereas for the less volatile chemicals, the situation is closer to heat transfer by conduction alone. Since the actual depth of the pool is a function of the evaporation rate, an average depth was used in this study for simplicity.

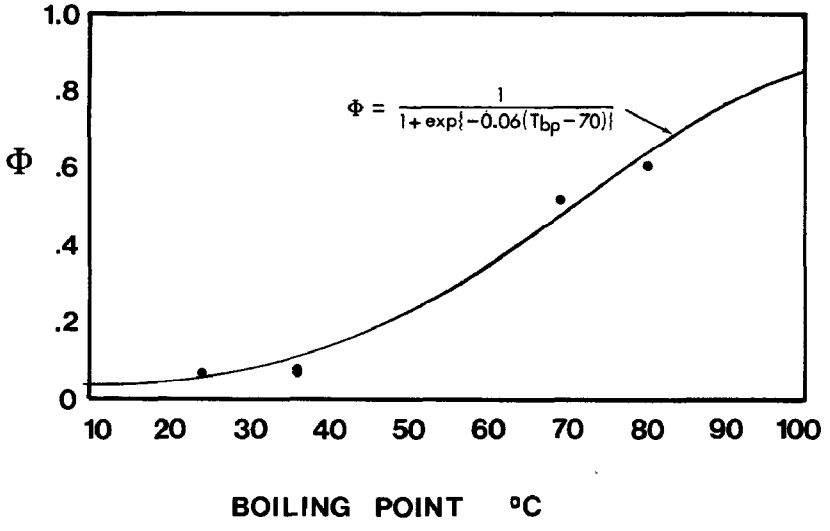

Fig. 5. Liquid resistance factor.

5.3 Ground conduction evaporation experiments

The average experimental evaporation rate, which included the effects of conduction from the ground, was compared to the predicted evaporation rates determined from the two evaporation models. The results are presented in Table 2, along with the air temperature, the duration of the experiment, and the initial volume of the chemicals used.

The results in Table 2 are similar to the results obtained in the first set of experiments (Table 1). Both models were able to predict the evaporation rate fairly accurately with the surface temperature method being the more accurate. The direct evaporation model was, again, found to underpredict the evaporation rate for the very volatile chemicals; pentane, and Freon 11. It should be

TABLE 2

Results and model predictions (kg/m^2 h) for ground conduction experiments

Exp. No.	Chemical	Air temp., °C	Initial volume, L	Time, (h)	Model predictions				Average evaporation rate
					Direct evap.	(%)	Surface temp.	(%)	
18	Toluene	25	4	3.5	5.42	(39)	4.95	(27)	3.90
19	Cyclohexane	29	4	1.67	9.92	(6)	10.44	(11)	9.38
20	Hexane	27	4	1.5	8.93	(23)	9.30	(28)	7.28
21	Pentane	23	7	1.07	15.90	(31)	22.45	(2)	23.00
22	Pentane	25	4	0.58	20.69	(24)	27.52	(2)	27.10
23	Freon 11	31	7	1.5	30.15	(14)	36.42	(4)	34.88

TABLE 3

Energy terms (kJ/m^2 h) for ground conduction experiments

Exp. No.	Chemical	Q_{sol}	$(Q_{atm} - Q_{sur})$	Q_{sen}	Q_{grd}	Q_{ev}
18	Toluene	3140	−410	−390	−180	2160
19	Cyclohexane	3220	17	620	330	4190
20	Hexane	2620	20	370	420	3430
21	Pentane	2330	320	3200	2530	8380
22	Pentane	3100	290	3300	3810	10490
23	Freon 11	3070	220	930	2580	6800

noted that the experimental evaporation rate in this set of experiments is the average evaporation rate for the experimental duration, unlike the steady state evaporation rate in the first set of experiments.

Since the average prediction error of the surface temperature model in both sets of experiments (with and without ground conduction) was nearly identical, it can be concluded that eqns. (11–15) were successful in quantifying the effect of ground conduction. Although the average error in the direct evaporation model increased slightly for the set of experiments involving ground conduction, this is not attributed directly to the introduction of the heat transfer from the ground since the same ground conduction equations were employed in both models.

The magnitude of the ground conduction and other energy terms is given in Table 3. These terms, with the exception of solar insolation, were determined from the surface temperature predicted by the surface temperature model.

It is clear that the thermal conduction from the ground accounts for a significant portion of the incoming energy for very volatile chemicals (experiments 21–23) and is comparable in magnitude to the sensible heat gain from the air for less volatile chemicals. The time dependence of Q_{grd} can be seen by the greater ground conduction heat transfer for experiment 22 (time period 0.58 h) as compared to experiment 21 (1.07 h). As expected, the effect of ground conduction, as well as heat transfer from the air and the evaporation energy is greater for chemicals of higher volatility.

The experiment involving toluene (experiment no. 18) illustrates the opposite of evaporative cooling, which may be termed, "solar heating" of the pool. This usually occurs when low volatility chemicals are exposed to high solar insolation, which results in higher pool temperatures, relative to the air temperature. Comparison of the experimental toluene pool temperatures with the air temperature confirmed this effect. Instead of energy being conducted to the pool from the air and ground, as in experiments no. 19–23, energy was lost from the toluene pool by these two routes. Both models included this effect for

this experiment by predicting an evaporation rate that corresponded to a surface temperature which was greater than the air temperature.

Finally, in the direct evaporation model, it was assumed that the net longwave energy contribution, $(Q_{atm} - Q_{sur})$, is relatively small and considered negligible. The results obtained from these set of experiments, although not conclusive, seem to justify this assumption. This radiative energy term, however, is still employed by the surface temperature model since the required computation does not significantly increase the complexity or the computation time.

5.4 Model application

Since both the direct evaporation and surface temperature models were able to estimate the evaporation rate within the accuracy required for chemical spills, either model could be employed in actual spill situations. The models may be used with confidence for liquids with boiling points which exceed 10°C below ambient temperatures. Caution should be applied when using these models outside this temperature range. Since the effects of boiling, freezing of the ground, and low vapor cloud formation are not included, these models should not be used for chemicals such as natural gas, chlorine and propane.

The main advantage of both models is that the amount of input data required is small, and readily obtainable. In terms of convenience, the direct evaporation method is the preferred model because it does not require a computer. It is therefore useful for the rapid prediction of the evaporation rate, and at locations where a computer cannot be used, such as at the spill site. On the other hand, since more accurate results were obtained using the surface temperature model, this method may prove to be valuable for those seeking a more thorough and accurate estimate. Therefore, both models are useful, and the model to use will likely depend on personal preference, accuracy desired, convenience, and application.

6 Conclusions

Two models, the "direct evaporation" equation and the "surface temperature" method have been developed, which predict the evaporation rate of pure volatile liquid chemicals resulting from ground spills. The models are relatively simple, based on available physical–chemical data, and include effects of variables such as evaporative cooling, solar insolation, and thermal conduction from the ground. The models are regarded as being applicable to liquids with boiling points in excess of 10°C below ambient temperatures.

Two sets of evaporation experiments were performed in which the predictions from the two evaporation models were compared with the experimental evaporation rate. In the first set, seven selected volatile chemicals were evaporated under varying environmental conditions with no thermal contribution

from the ground. This heat transfer from the ground was incorporated in the second set of experiments in which five of the seven chemicals were employed. The two models showed satisfactory agreement with the experimental evaporation rates for both sets of experiments. The difference between the model predictions and the experimental evaporation rates for these experiments ranged from 0 to 40% for the first set and 6 to 39% for the second set for the direct evaporation model, and 1 to 32% and 2 to 27% for the surface temperature model.

Although slightly more accurate results were obtained for the surface temperature method, the direct evaporation equation is preferred because of its simplicity and convenience. It is probable that personal preference, the value of the application and the desired accuracy will dictate which model should be employed in the estimation of the evaporation rate for spill situations.

7 Acknowledgements

The authors are grateful to Environment Canada, Transport Canada, and Natural Sciences and Engineering Research Council for financial support, and to the Atmospheric Environment Services Branch in Downsview, Ontario for permission to conduct experiments at their site in Woodbridge, Ontario.

List of symbols

a	vapor pressure constant
b	vapor pressure constant
B	atmospheric radiation factor
B_o	Bowen's ratio
c	vapor pressure constant
C	cloud cover factor
C_{p_a}	heat capacity of air (kJ/mol K)
C_{p_g}	heat capacity of ground (kJ/kg K)
$\bar{d}$	average depth of pool (m)
D	declination
D_{ab}	diffusivity in air (cm^2/s)
e	emissivity
E	evaporation rate per unit area (g/m^2 h)
h_{grd}	heat transfer coefficient of the ground (kJ/m^2 h K)
h_{liq}	heat transfer coefficient of the chemical (kJ/m^2 h K)
H_v	heat of vaporization (kJ/mol)
k	mass transfer coefficient (m/h)
k_{grd}	thermal conductivity of the ground (kJ/m h K)
LA	latitude (degrees)
LCT	local standard time (h)

LG	longitude (degrees)
M	molecular weight (g/gmol)
N	day number
P^*	saturated vapor pressure (Pa)
$P(t)$	vapor pressure at temperature t (Pa)
P_{atm}	atmospheric pressure (Pa)
P_a	partial pressure in air (Pa)
P_s	partial pressure at the surface (Pa)
Pr	Prandtl number
Q_{atm}	long-wave radiation from the atmosphere (kJ/m^2 h)
Q_{ev}	evaporation energy (kJ/m^2 h)
Q_{grd}	conduction energy from the ground (kJ/m^2 h)
Q_{sen}	sensible heat from the air (kJ/m^2 h)
Q_{sol}	net solar insolation (kJ/m^2 h)
Q_{sur}	long-wave radiation emitted by the pool (kJ/m^2 h)
Q_t	increase in energy stored in the pool (kJ/m^2 h)
r	reflectivity of long-wave radiation
R	gas constant (Pa m^3/mol K)
S	slope of vapor pressure curve at air temperature (Pa/K)
SA	solar altitude (degrees)
Sc	Schmidt number
t_{bp}	boiling point (°C)
T	absolute temperature (K)
TZ	time zone factor
U	10 m wind speed (m/h)
U_{grd}	overall heat transfer coefficient of ground (kJ/m^2 h K)
U_{liq}	heat transfer coefficient between pool and air (kJ/m^2 h K)
X	pool diameter or length (m)
Z	factor in Bowen's ratio (Pa/K)

Greek symbols

α	thermal diffusivity of the ground (m^2/h)
θ	time after the spill (h)
ρ_a	molar density of air (mol/m^3)
ρ_g	density of ground (kg/m^3)
σ	Stefan–Boltzmann constant (kJ/m^2 h K^4)
ϕ	liquid resistance factor
ν	kinematic viscosity of air (cm^2/s)
β	Z/S ratio

References

1 P. Kawamura and D. Mackay, The evaporation of volatile liquids, Technical Services Branch, EPS, Report EE-59, 1985.
2 C.G. Whitacre and M.M. Myirski, Computer program for chemical hazard protection, ARCSL-TR-822014, 1982.
3 H.J. Clewell, A simple formula for estimating source strengths from spills of toxic liquids, ESL-TR-83-03, 1983.
4 Air Weather Service, Calculation of toxic corridors, AWS Pamphlet, 105-57, 1978.
5 W. Stiver and D. Mackay, Evaporation rate of spills of hydrocarbons and petroleum mixtures, Env. Sci. Technol., 18 (1984) 834.
6 M.T. Fleischer, Spills — An evaporation/air dispersion model for chemical spills on land, Shell Dev. Co., PB 83109470, 1980.
7 G. Ille and C. Springer, The evaporation and dispersion of hydrazine propellants from ground spills, CEEDO-TR-78-30 AD-A059407, 1978.
8 J.M. Raphael, Prediction of temperature in rivers and reservoirs, Proc. Amer. Soc. Civ. Eng., J. Power Div., 88 P02, 1962.
9 D. Mackay and R.S. Matsugu, Evaporation rate of hydrocarbon spills on water and land, Can. J. Chem. Eng., 5 (1973) 434.
10 J.P. Holman, Heat Transfer, McGraw Hill, New York, 1976.
11 H.L. Penman, Natural evaporation from open water, bare soils and grass, Proc. R. Soc. London, Ser. A., 193 (1948) 120–146.
12 W.H. Brutsaert, Evaporation into the Atmosphere, D. Reidel, Dordrecht, The Netherlands, 1982.
13 L.J. Thibodeaux, Chemodynamics, John Wiley and Sons, New York, 1979.
14 L.D. Baver, W.H. Gardner and W.R. Gardner, Soil Physics, John Wiley and Sons, New York, 1972.
15 P.J. Lunde, Solar Thermal Engineering, John Wiley and Sons, New York, 1980.

Appendix

To summarize the models and their procedure, a sample calculation for experiment no. 21 is illustrated.

A. Spill data

Chemical	Pentane
Spill volume	7 L
Spill area	0.162 m^2
Diameter of pool, X	0.454 m
Spill date	July 30
Average spill time	9:15 EST
Spill duration, θ	1.07 h
Spill location	Toronto, Ontario (longitude 80°, latitude 44°)
Air temperature	23°C
Cloud cover factor, C	2 (20%)
Relative humidity	63%
10 m wind speed, U	17,800 m/h
Ground description	water-saturated sand

B. Physical–chemical properties

B1: Pentane

Molecular weight, M	72
Boiling point, t_{bp}	36 °C
Liquid thermal conductivity, k_{liq}	0.41 kJ/m h °C
Heat of vaporization, H_v	27.4 kJ/mol
Diffusivity in air [13], D_{ab}	0.071 cm^2/s

Vapor pressure, P^*:

$\log_{10}P^* = a - (b/(t+c))$, where P^* has units of mmHg and t in Celsius: for pentane, $a = 6.85296$, $b = 1064.84$, and $c = 233.01$

B2: Other properties

Kinematic viscosity of air [13]	0.15 cm^2/s
Thermal conductivity of saturated sand [14], k_{grd}	7.5 kJ/m h °C
Thermal diffusivity of sand	0.00252 m^2/h

C. Preliminary calculations

C1. Solar insolation

Estimating the solar insolation using eqn. (2) requires the determination of the solar altitude, which is given by the following expresion [8]:

$$\sin(SA) = \sin(LA)\ \sin(D) + \cos(LA)\ \cos(D)\ \cos(h)$$

where LA is the latitude in degrees, D is the declination, and h is the hour angle in degrees. Declination is evaluated by [15]:

$$D = 23.45 \sin(0.97(N-80))$$

where N is the day number of the year. The hour angle is approximately [15]:

$$h = 15 \text{ abs } [12 - (LCT + TZ - (LG/15))]$$

in which LCT is the local standard time in hours, TZ is the time zone factor, and LG is the longitude, in degrees. For North America, the time zone factors are [15]: EDT, +4; EST, +5; CST, MDT, +6; MST, PDT, +7; PST, +8.

For the spill situation: $LCT = 9.25$ EST, $TZ = +5$, $N = 211$, $C = 2$, $D = 23.45 \sin(0.97(211-80)) = 18.7$, and $h = 15$ abs $[12 - (9.25 + 5 - (80/15))] = 46.2$. Thus, $\sin(SA)$ is:

$$\sin(SA) = \sin(44)\ \sin(18.7) + \cos(44)\ \cos(18.7)\ \cos(46.2)$$

$\sin(SA) = 0.695$, i.e. SA is 44°

From equation 2, the solar insolation is:

$$Q_{sol} = 4000\ (1 - 0.0071\ C^2)\ (\sin(SA) - 0.1)$$
$$= 2311\ \text{kJ/m}^2\ \text{h}$$

C2. Mass transfer coefficient

The mass transfer coefficient is given by eqn. (6):

$$k = 0.029\ U^{0.78}\ X^{-0.11}\ Sc^{-0.67}$$

The Schmidt number is:

$$Sc = \nu / D_{ab} = 0.15/0.071 = 2.11$$

is therefore:

$$k = 0.029\ (17800)^{0.78} (0.454)^{-0.11} (2.11)^{-0.67}$$
$$k = 39.7\ \text{m/h}$$

C3. Ground heat transfer coefficients

To calculate the overall ground heat transfer coefficient, U_{grd}, h_{grd}, and h_{liq} must be determined.

i. From eqn. (11):

$$h_{grd} = 2\ k_{grd}\ (\theta / \eta p \alpha)^{0.5/\theta}$$
$$= 2(7.5)\ (1.07/3.14*0.00252)^{0.5}/1.07 = 163\ \text{kJ/m}^2\ \text{h}\,^\circ\text{C}$$

ii. From eqn. (13);

$$h_{liq} = k_{liq} / (\phi \bar{d})$$

where $\phi = 1/[1 + \exp(-0.06(t_{bp} - 70))]$ (eqn. 14)

$$\phi = 0.12$$

$$\bar{d} = d\ (\text{initial})/2 = 0.043/2 = 0.022\text{m}$$

It follows that

$$h_{liq} = 0.41/(0.12*0.022) = 155\text{kJ/m}^2\ \text{h}\ ^\circ\text{C}$$

iii. Combining the two heat transfer coefficients (eqn. 12):

$$1/U_{grd} = (1/h_{liq}) + (1/h_{grd})$$

$$U_{grd} = 79.4\ \text{kJ/m}^2\ \text{h}\ ^\circ\text{C}$$

D. Model calculation

D1. Direct evaporation model

The evaporation rate is given by eqn. (23):

$$E=(S/(Z+S))E_r+(Z/(Z+S))E_a$$

The individual terms are calculated as follows:

i. From eqn. (21)

$$E_r=Q_{sol}\ M/H_v=2311\times 72/27.4=6073\ \text{g/m}^2\ \text{h}$$

ii. From eqn. (18)

$$Z=3650\ Sc^{0.67}/H_v+U_{grd}\ R\ T/(k\ H_v)$$

$$=3650\ (2.11)^{0.67}/27.4+79.4\times 8.314\times(23+273)/(39.7\times 27.4)$$

$$=400\ \text{Pa/K}$$

iii. From eqn. (19):

$$S=(\mathrm{d}P^*/\mathrm{d}T)_{T_a}$$

For vapor pressure equation of the form:

$$\log_{10}P^*=a-(b/(t+c))$$

$$\mathrm{S}=133[2.3\mathrm{b}/(\mathrm{t}+\mathrm{c})^2]\ \exp\ [2.3(a-(b/(t+c))]=2437\ \text{Pa/K}$$

(133 is the pressure conversion factor to Pa.)

iv. The term E_a can be deduced from eqn. (22):

$$E_a=k\ M\ P\ (T_a)/(R\ T)$$

$$P(T_a)=133\ \exp[2.3(a-(b/(t_a+c))]=65225\ \text{Pa}$$

$$E_a=39.7\times 72\times 65225/[8.314(23+273)]=75760\ \text{g/m}^2\ \text{h}$$

The evaporation rate can now be calculated using eqn. (23)

$$E=[2437/(2437+400)]\ 6073+[400/(2437+400)]\ 75760$$

$$=15897\ \text{g/m}^2\ \text{h}$$

The predicted evaporation rate is 15.90 kg/m^2 h. The experimental rate was 23.00 kg/m^2 h.

D2. Surface temperature model

To determine the surface temperature of the pool, which is required to evaluate the evaporation rate, the variables in eqn. (27) must be evaluated and the

equation solved. The parameters yet to be calculated are the atmospheric radiation factor, B, and the heat transfer coefficient, U_{liq}.

i. Atmospheric radiation factor. This term is evaluated from the relative humidity, RH. RH = vapor pressure of water in atmosphere/vapor pressure of saturated air.

The vapor pressure of saturated air at the air temperature of 23 °C is 29 mbars [8]. The vapor pressure of water in the atmosphere is $0.63 \times 29 = 18$ mbars. From Fig. 2, the atmospheric radiation factor is 0.84.

ii. Heat transfer coefficient, U_{liq}. The heat transfer coefficient is identified by eqn. (9). Employing the values for the Prandtl number and the product of the molar density of air and the heat capacity of air, as given in Section 2, eqn. (9) reduces to:

$$U_{liq} = 1.2\, k\, (Sc)^{0.67}/0.804$$

For this experiment, U_{liq} is:

$$U_{liq} = 1.2 \times 39.7 \times (2.11)^{0.67}/0.804 = 98 \text{ kJ/m}^2 \text{ h °C}$$

The energy balance was written as (eqn. (26)):

$$Q_{sol} + Q_{atm} + T_a(U_{liq} + U_{grd}) = T_s\,(U_{liq} + U_{grd}) + kH_v P(T_s)/(RT_s) + e\sigma T_s^4$$

This equation may now be expressed as:

$$2311 + (1 - 0.03)2.04 \times 10^{-7}(296)^4 + 296(102 + 79.4)$$
$$= T_s(102 + 79.4) + 39.7 \times 27.4 \times P(T_s)/8.314\, T_s + 0.97 \times 2.04 \times 10^{-7}\,(T_s)^4$$

in which $P(T_s) = 133 \exp\{2.3\{a - [b/(T_s - 273 + c)]\}\}$

This equation may be solved for T_s by a standard root determining procedure. The root, or the surface temperature was found to be −8.2 °C.

The evaporation rate can now be determined using eqn. (5) and $T_s = 264.8$ K.

$$E = k\,M\,P(T_s)/(R\,T_s) = 22450 \text{ g/m}^2 \text{ h}$$

The predicted evaporation rate is 22.45 kg/m^2 h.